Critical Reflux, Parametric Sensitivity, and Hysteresis in Azeotropic Distillation of Isopropyl Alcohol + Water + Cyclohexane

ARTICLE · JUNE 1998

2 AUTHORS, INCLUDING:

David Shan Hill Wong
National Tsing Hua University
151 PUBLICATIONS **2,551** CITATIONS

Critical Reflux, Parametric Sensitivity, and Hysteresis in Azeotropic Distillation of Isopropyl Alcohol + Water + Cyclohexane

C. J. Wang and D. S. H. Wong*

Department of Chemical Engineering, National Tsing Hua University, Hsinchu, Taiwan 30043

I-L. Chien

Department of Chemical Engineering, National Taiwan University of Science and Technology, Taipei, Taiwan 10672

R. F. Shih, W. T. Liu, and C. S. Tsai

Pilot Plant Division, Union Chemical Laboratories, Industrial Technology Research Institute, Hsinchu, Taiwan 30043

In this work, the characteristics of heterogeneous azeotropic distillation of isopropyl alcohol (IPA) + water (H_2O) with cyclohexane (CyH) as an entrainer were investigated. Critical reflux, parametric sensitivity, and hysteresis were found by theoretical analysis and supported by experiment using a laboratory-scale sieve plate distillation column. At each given reflux rate, there are two branches of stable steady states as reboiler duty varies, one with desirable purity and another with almost no separation. The highest attainable purity is achieved at a specific reboiler duty. Beyond this duty there is a catastrophic loss in IPA purity. At higher refluxes, the temperature profiles of the column with highest attainable purity pass around the IPA + CyH azeotrope. A plateau at 69.3 °C characterizes this type of profile. There is little change of highest attainable IPA purity as reflux varies. When reflux is reduced below a critical value, the temperature profile of the column with highest attainable purity passes around the IPA + H_2O azeotrope. The highest attainable IPA purity decreases substantially as reflux is reduced. The critical reflux represents an operating state that achieves high IPA purity with minimum energy consumption. Furthermore, at a given pair of reflux and reboiler duty, the steady-state temperature profile that achieves good separation is not unique. The exact position of the temperature front can be fixed at any position inside the column using a cyclic series of step changes in reboiler duty. This hysteresis phenomenon is attributable to changes in entrainer inventory inside the column.

Introduction

Azeotropic distillation is a special distillation process developed to solve the problems of close relative volatility and breaking azeotrope. A recent review by Widagdo and Seider (1996) showed that parametric sensitivity, multiple steady states, long transient, and nonlinear dynamics were found by many authors using theoretical models and computer simulation. Magnussen et al. (1979) was the first to find multiple steady states for an ethanol + benzene + water system using steady-state simulation. The phenomenon was confirmed by many authors using steady-state or dynamic simulation (Prokopakis et al., 1981; Prokopakis and Seider, 1983a,b; Kovach and Seider, 1987a,b; Widagdo et al., 1989, 1992; Cairns and Furzer, 1990a−c; Rovaglio and Doherty, 1990; Rovaglio et al., 1993). Pham et al. (1989) found that small changes in the impurities of the bottom product will induce different design distillation paths and explained the phenomena with residual curve map analysis (Pham and Doherty, 1990). Bekiaris et al. (1993, 1996) proposed a geometric analysis for the existence of multiple steady states at infinite reflux and with infinite numbers of plates, with the distillate as the bifurcation parameter. The results were confirmed by rigorous analysis of a constant-molar-overflow material balance model. Güttinger et al. (1997) confirmed the analytical results experimentally for a homogeneous system. However, systematic experimental investigation of heterogeneous azeotropic distillation is still relatively scarce. Kovach and Seider (1987a) performed a step feed rate change test for an industrial column for dehydrating secondary butyl alcohol (SBA) using di-*sec*-butyl ether (DSBE) as the entrainer. Erratic behavior was found and attributed to parametric sensitivity, but the results were inconclusive. Müller et al. (1997) compared data obtained by an equilibrium stage model for an ethanol + cyclohexane + water column with a laboratory tray column. The experimental composition profiles obtained at infinite reflux and a given production case agree with the model with an assumption of 70% overall efficiency. A very recent publication (Müller and Marquardt, 1997) reported evidence of multiple steady states for the system.

In this work, residue curve, bifurcation analysis, and dynamic simulation were used to investigate the steady-state and dynamic behavior of an isopropyl alcohol (IPA), cyclohexane (CyH), and water (H_2O) heterogeneous azeotropic column. Results of theoretical analysis were used to explain experimental phenomena observed

* Corresponding author. Fax/Tel: 3-5721694. E-mail: dshwong@che.nthu.edu.tw.

S0888-5885(97)00855-5 CCC: $15.00
Published on Web 06/16/1998

Table 1. Coefficients for Antoine Equations

	a	*b*	*c*
IPA	11.043	−3109.3	−73.5
CyH	9.169	−2794.6	−49.1
water	11.964	−3984.9	−39.7

Table 2. Enthalpy Coefficients (T_0 = 298 K; $h(H)$, J/mol)

	liquid enthalpy				
	h_0	h_1	h_2	$h_3 \times 10^3$	$h_4 \times 10^6$
IPA	0	38.89	1.045	−0.5202	0
CyH	0	407.4	−3.860	10.65	0
water	0	50.83	0.213	−0.6312	0.6486

	vapor enthalpy				
	H_0	H_1	$H_2 \times 10^2$	$H_3 \times 10^4$	$H_4 \times 10^8$
IPA	45588	17.614	63.368	−5.16	14.506
CyH	32495	−55.334	123.59	−7.85	0
water	44529	33.913	−0.3014	0.152	−0.4857

in a laboratory-scale sieve plate distillation column equipped with temperature sensors, sampling ports, and flow controllers.

Analytical Tools

Thermodynamic Models. Vapor pressures were computed by the Antoine equation:

$$\ln P_i^s(T) = a_i + \frac{b_i}{T + c_i} \tag{1}$$

where T is in K and P_i^s is in bar. The Antoine coefficients come from Reid et al. 1988 (Table 1). The enthalpies of liquid and vapor are assumed to be a function of temperature only and can be expressed by a fourth-order polynomial.

$$h(H)_i(T) = h(H)_{i0} + h(H)_{il}(T - T_{0i}) + \frac{h(H)_{i2}}{2}(T^2 - T_{0i}{}^2) + \frac{h(H)_{i3}}{3}(T^3 - T_{0i}{}^3) + \frac{h(H)_{i4}}{4}(T^4 - T_{0i}{}^4) \tag{2}$$

The enthalpy coefficients are from Reid et al. (1988), Prokopakis and Seider (1983a), and Prokopakis et al. (1981) (Table 2). The vapor phase was assumed to be ideal. A NRTL model was used to describe nonideality of the liquid. To obtain a set of parameters capable of consistently describing binary and ternary, vapor−liquid (VLE) and liquid−liquid equilibrium (LLE) data, the Bender and Block method (Bender and Block, 1975) was used to regress experimental data. For the mixture IPA (1) + CyH (2) + Water (3) at 25 °C, the 2−3 pair is only partially miscible; the other two pairs are completely miscible. The binary parameters B_{ij} for the 1−2 and 1−3 pairs are obtained by fitting binary VLE data (Gmehling and Onken, 1977) with $\alpha_{12} = \alpha_{13} = 0.5$. At each specified α_{23}, B_{23} and B_{32} were fit using mutual solubility data (Sørensen and Arlt, 1979). Finally, the ternary vapor−liquid and liquid−liquid equilibrium data (Verhoeye, 1968) was used to determine an optimal value of α_{23} (listed in Table 3). The tie-lines and lower binodal region of the ternary system agree well with experiment, but the plait point is higher and the near-critical region is larger.

Residual Curve Map. A residue curve map records the change of the liquid composition with time in a simple distillation. The governing equations (Pham and Doherty, 1990) are of the form

Table 3. Parameter Values for the NRTL Model (1, IPA; 2, CyH; 3, Water)

i, *j*	B_{ij}	B_{ji}	α_{ij}
1, 2	294.6	622.5	0.5
1, 3	185.4	777.3	0.5
2, 3	1629	2328	0.242

$$\frac{dx_i}{d\xi} = x_i - y_i \tag{3}$$

where x and y are the compositions of the liquid and vapor phases and ξ is the dimensionless time. A fourth-order Runge−Kutta integration was used to calculate the liquid composition loci. At each time step, the tangent plane splitting check (Michelen, 1982) was performed, followed by either VLE or VLLE bubble-point calculation.

Bifurcation Analysis. Consider an azeotropic distillation column which has 28 stages, including condenser−decanter (stage 1) and reboiler (stage 28) with the feed stream at stage 4. The feed flow rate is 1 mol/min, containing 69 mol % IPA and 31 mol % H_2O. The entrainer makeup flow rate is 0.03 mol/min and adds to the decanter. The feed temperature is 298 K. The pressure drop inside the column is assumed to be zero. Constant molar overflow (CMO) and ideal tray efficiency are assumed. Heterogeneous liquid-phase split was allowed in any stage. Following Schuil and Bool (1985), the steady-state balance equations were expressed as the "overall" liquid composition, and K-values were defined as the average properties of the two coexisting liquid phases:

$$\bar{x}_{ij} = \beta_j x'_{ij} + (1 - \beta_j)x''_{ij} \qquad \frac{1}{\bar{K}_{ij}} = \frac{\beta_j}{K'_{ij}} + \frac{1 - \beta_j}{K''_{ij}} \tag{4}$$

The tangent plane analysis (Michelsen, 1982) was used to check for possible phase splitting for the "overall" liquid composition. Bubble-point or VLLE calculations were used to calculate the K-values accordingly. AUTO, a software package developed by Doedel and Wang (1994), was used to perform bifurcation analysis of the steady-state material balance and equilibrium relation. Reflux and vapor flow rates are the two system parameters. Numerical derivatives with respect to average composition and system parameters were used. The effect of vapor flow rate on the steady-state behaviors of the system can be traced, with reflux being held constant.

Dynamic Simulation. The column specifications were the same as those for bifurcation analysis, except that the CMO assumption was removed. In addition to the "overall" liquid composition and K-values in eq 4, average liquid flows and holdup were also defined:

$$\bar{M}_j = \frac{M'_j}{\beta_j} = \frac{M''_j}{1 - \beta_j} \qquad \bar{L}_j = \frac{L'_j}{\beta_j} = \frac{L''_j}{1 - \beta_j} \tag{5}$$

The material balance equation was integrated by a third-order semiimplicit Runge−Kutta method to obtain "overall" liquid flow rates and liquid compositions. The tangent plane analysis (Michelsen, 1982) was used to check for possible phase splitting for a given average composition. Bubble-point or VLLE calculations were used to update the average K-values. Average holdups

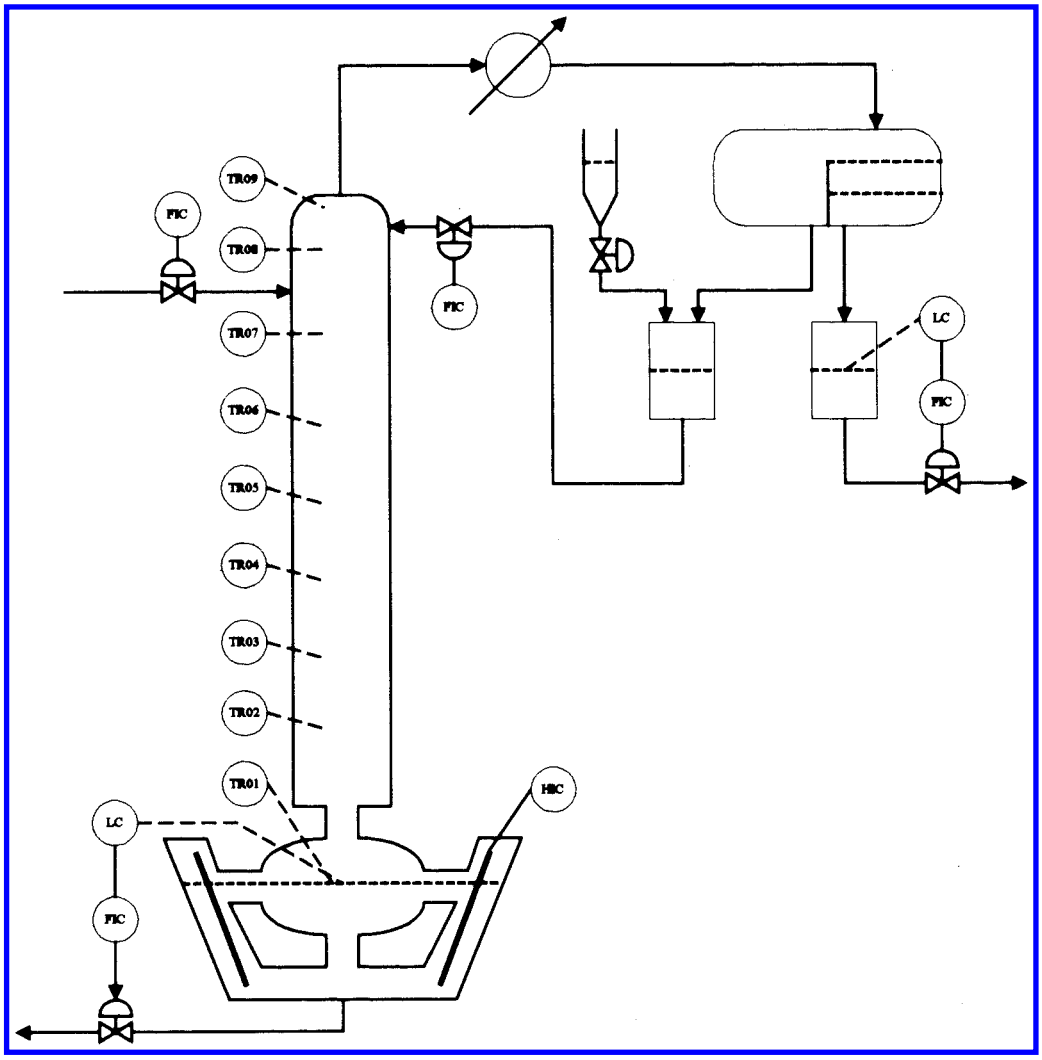

Figure 1. Schematic diagram of the experimental device.

were calculated by Frances' weir equation and average liquid flow. Vapor flows were obtained by enthalpy balance. Details of the simulation algorithm were furnished in Wong et al. (1991).

A feed flow rate of 1 mol/min was used in all of our simulations. This feed is of the same order of magnitude as the feed in our experiment. The decanter holdup and weir constants were set so that ratios of tray and decanter holdup to the feed rate would be the same order of magnitude as those in our experiment. The decanter aqueous-phase level was perfectly controlled by the aqueous distillate draw rate. The decanter organic-phase level was maintained by on−off control using entrainer makeup. The two operating variables are the organic reflux rate and reboiler duty.

Experimental Setup

The schematic illustration of the experimental setup is shown in Figure 1. The main structure of the experimental device is a Pyrex glass sieve tray column sheathed with a glass tube. The compartment between the distillation column and the outer glass tube is a vacuum that keeps the column adiabatic. The diameter of a plate is 5 cm. Nine temperature measurement and sampling ports, TR01 to TR09, are located at plates from bottom to top. Plate 1 is the first plate at the top of the column. A water manometer measures the pressure drop of the column. There is an opening at the top of the column to maintain atmospheric pressure. The organic liquid and aqueous liquid overflow to two 2-L surge tanks. The reboiler is a V-shaped quartz tube capable of supplying 4 kW. During operation, the level of the aqueous surge tank was controlled by the aqueous distillate, and the organic surge tank level was maintained by on−off control using entrainer makeup. The average consumption rate of the makeup was found to be about 1−2 cm^3/min. The operating variables are organic reflux rate and reboiler heat duty. A gas chromatograph (Shimadzu model GC-8A) with a chromosorb-101 column was used to analyze the samples.

Results and Discussion

Residual Curve Map. Figure 2 is the residue curve map of a IPA + CyH + H_2O system shown together with the immiscible region at 25 °C. The distillation boundaries divided the whole composition space into three distillation regions. The bottom product is pure IPA at one corner of the top region. The composition of the vapor distillate approaches the ternary azeotrope, which is another corner of the top region. Therefore, only the top region is of concern in this work. However, many different paths can connect the two corners of this top region. A small change in the composition of the distillate will result in an entirely different distillation

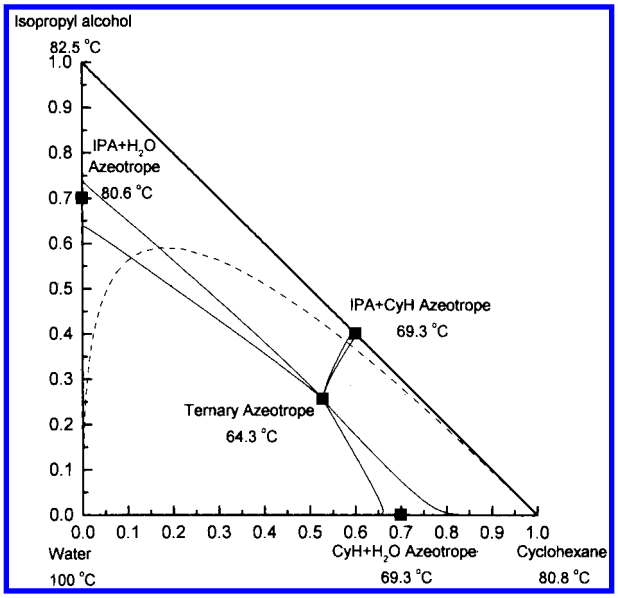

Figure 2. Residue curve map of the IPA + CyH + H_2O system.

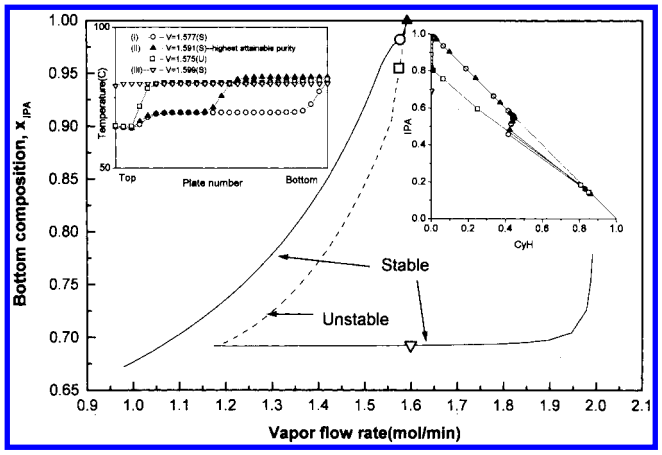

Figure 3. Bifurcation analysis at reflux = 1.0 mol/min.

path. This is why azeotropic distillation has the characteristics of multiple steady-state and parametric sensitivity.

Bifurcation Analysis. Figure 3 shows the relationship between bottom composition (IPA) and vapor boilup rate, with reflux being fixed at 1.0 mol/min. There exist three branches of steady states when the vapor flow rate ranges from about 1.2 to 1.6 mol/min at this reflux. The upper high-purity branch and the lower low-purity branch are stable, while the middle is unstable. The vapor boilup rate achieving the highest attainable purity (0.999) is at about 1.591 mol/min. Along the top branch, for a vapor boilup rate much smaller than 1.591 mol/min, a profile of type I was found. As we travel along the top branch by increasing the vapor rate, the purity of IPA increases and profiles of type II could be obtained. If the vapor boilup rate is increased beyond 1.591 mol/min, the profile would go through a catastrophic change to a type III profile. The composition profiles at the three vapor flow rates are plotted on a triangular diagram in Figure 3. Profiles I and II pass from the IPA corner around the IPA + CyH azeotrope toward the ternary azeotrope. The immiscible region is avoided inside the column. Profile III shrinks to a single point around the feed (IPA + H_2O azeotrope). The entrainer is completely stripped out of the column, and there is no separation at all.

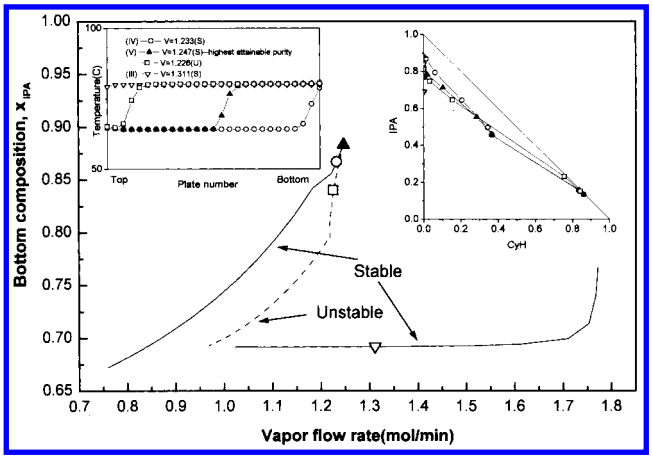

Figure 4. Bifurcation analysis at reflux = 0.78 mol/min.

A similar phenomenon is observed when the reflux is reduced to 0.78 mol/min as shown in Figure 4. There exist three branches of steady states when the vapor flow rate ranges from about 0.8 to 1.6 mol/min at this reflux. The upper stable branch achieves some separation and the lower stable branch achieves little separation, while the middle is unstable. The vapor boilup rate achieving the highest attainable purity (0.88) is about 1.247 mol/min. Along the top branch, for a vapor boilup rate much smaller than 1.247 mol/min a profile of type IV was found. As we increase the vapor rate, the purity of IPA increases and profiles of type V could be obtained. If the boilup rate is increased beyond 1.247 mol/min, the profile would go through a catastrophic change to a type III in the lower low-purity branch. Profiles IV and V start from the IPA corner and pass through the IPA + H_2O azeotrope toward the ternary azeotrope. Therefore, the top part of the column is inside the immiscible region and liquid-phase splitting should be observed.

The system exhibits multiple steady states and parametric sensitivity at both refluxes. However, there is a difference between them in the column profile and the highest attainable purity. At reflux = 1.0 mol/min, the highest attainable purity of IPA is 0.999. Profile II shows a 69.3 °C plateau. The distillation path connects the IPA corner with the ternary azeotrope corner by passing around the IPA + CyH azeotrope. However, for reflux = 0.78, the highest attainable purity of IPA is only 0.88. Profile V shows no plateau at 69.3 °C. The distillation path connects the IPA corner with the ternary azeotrope corner by passing around the IPA + H_2O azeotrope. Moreover, this profile is characterized by many heterogeneous stages at the top.

Müller and Marquardt (1997) reported that profiles similar to II−III, and V can be obtained at a given heat duty and distillate draw for an ethanol + cyclohexane + water system where types II and III are stable solutions and type V belongs to an unstable branch. This corresponds to the high reflux situation in our analysis. In Figure 3, a type V profile can be found along the unstable branch. In Figure 4, at a smaller reflux, the profile on the stabletop high-purity branch becomes type V instead of type II. At low reflux there is not sufficient entrainer inside the column to maintain a type II profile.

At each specified reflux, there will be a corresponding vapor flow rate that gives the highest purity of IPA. The collection of these points forms the optimum operation line. Figure 5 shows the relation of maximum attainable purity with reflux and vapor flow rate. The

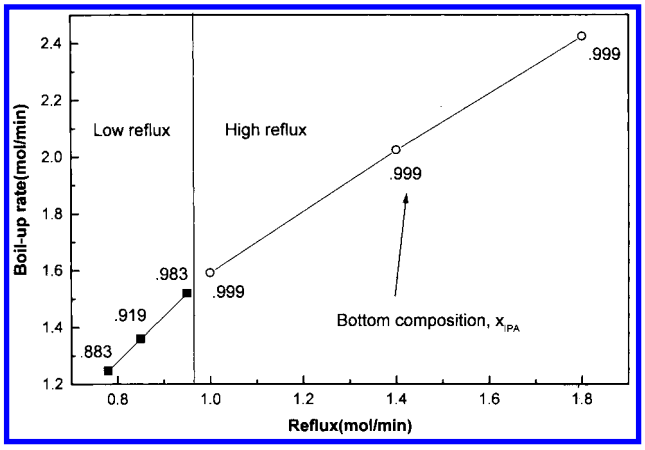

Figure 5. Optimum operation line for feed = 1.0 mol/min.

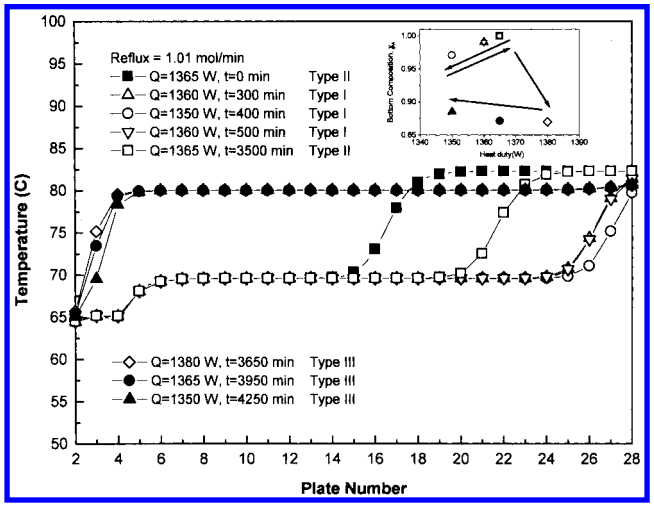

Figure 6. Steady-state temperature profiles (I−III) and hysteresis at reflux = 1.0 mol/min obtained by dynamic simulation.

relation clearly divides a high reflux region and a low reflux region. In these two regions, the relations of maximum attainable purity with reflux and vapor flow rate are both approximately linear but have different slopes. A critical point exists at which the column profile that achieves highest IPA purity will change from type II to type V. The purity of IPA decreases rapidly once reflux and vapor boilup are reduced below this critical point.

From a design standpoint, it is desirable that a column should operate at the minimum reflux and boilup rate at which a desired purity is achieved. If the purity objective of IPA is stringent, the critical point becomes a desirable operating point. The purity of IPA would not increase appreciably beyond this point. Operating at higher reflux and boilup rates may be more robust in terms of meeting quality specifications, but only at the expense of increased energy cost. Control problems associated with operating at just above the critical point will be discussed in a subsequent publication.

Dynamic Simulation. In Figure 6, a steady-state temperature profile (type II) obtained using the dynamic simulation model is shown. The reflux is about 1 mol/min, and the heat duty is 1365 W. The purity of the IPA product is 0.999, with impurity being cyclohexane. Its distillation path passes around the IPA + CyH azeotrope. If the reboiler duty is decreased from 1365 to 1360 W, a profile that is of type I is reached in 300 min. The plateau of 83 °C at the bottom of the column

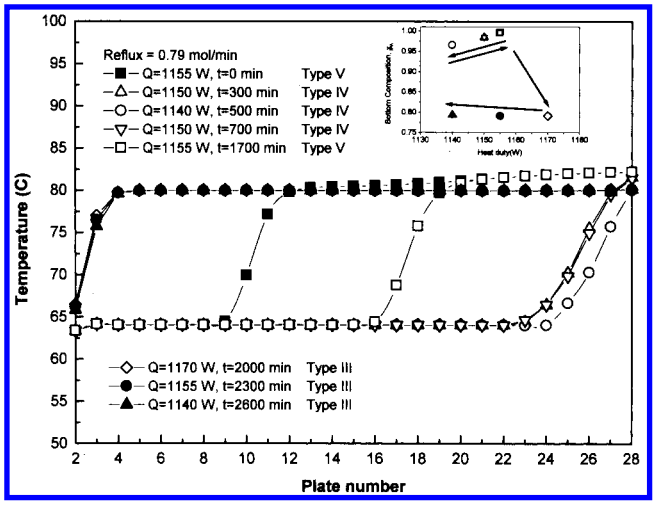

Figure 7. Steady-state temperature profiles (III−V) and hysteresis at reflux = 0.78 mol/min obtained by dynamic simulation.

almost vanishes completely. However, an IPA purity of 0.99 and a bottom temperature of 82 °C are still maintained. If the reboiler duty is further reduced from 1360 to 1350 W, a new steady-state profile of type I is reached in 100 min. If the reboiler duty is step increased from 1350 to 1360 W, the original type I profile is recovered in 100 min. However, if the reboiler duty is changed to 1365 W again, an extremely long transient of more than 3000 min is observed. Although a type II profile is recovered, the location of the temperature front differs from the original profile. A "hysteresis" phenomenon is observed. Upon further increase of the heat duty to 1380 W, a steady-state column profile of type III is reached within 150 min. The separation effect of the column is suddenly lost. This corresponds to a jump from a steady state on the upper high-purity branch to a steady state on the lower low-purity branch of the bifurcation analysis diagram in Figure 3. The system shows extreme parametric sensitivity at this point. After achieving a type III profile, the heat duty was reduced back to 1365 W for 300 min and then reduced further to 1350 W for another 300 min. There was essentially no change in the temperature profile. Thus, output steady-state multiplicity could be established at these heat duties (of types I and III at 1350 W and of types II and III at 1365 W). Müller and Marquardt (1997) reported similar results as hysteresis due to output multiplicity.

If the reflux is reduced to 0.79 mol/min, three different steady states (III, IV, and V) are also found (Figure 7). The respective reboiler duties are 1140, 1155, and 1170 W. For steady state V, the distillation path passes around the IPA + H_2O azeotrope and the purity of the IPA product is 0.99, with impurity being water. For profiles IV and V, there exist heterogeneous liquid phases in the top section of the column. The "hysteresis" phenomenon is also observed for the lower reflux. Similarly, there will be a sudden jump from type IV to type III profile if we increase the heat duty beyond a certain point to 1170 W. After achieving a type III profile, the heat duty was first reduced back to 1155 W for 300 min and then reduced further to 1140 W for another 300 min. There was essentially no change in the temperature profile. Therefore, at 1155 W, two types of steady states with profiles of types V and III were found, while at 1140 W, two types of steady states with profiles of types IV and III were found.

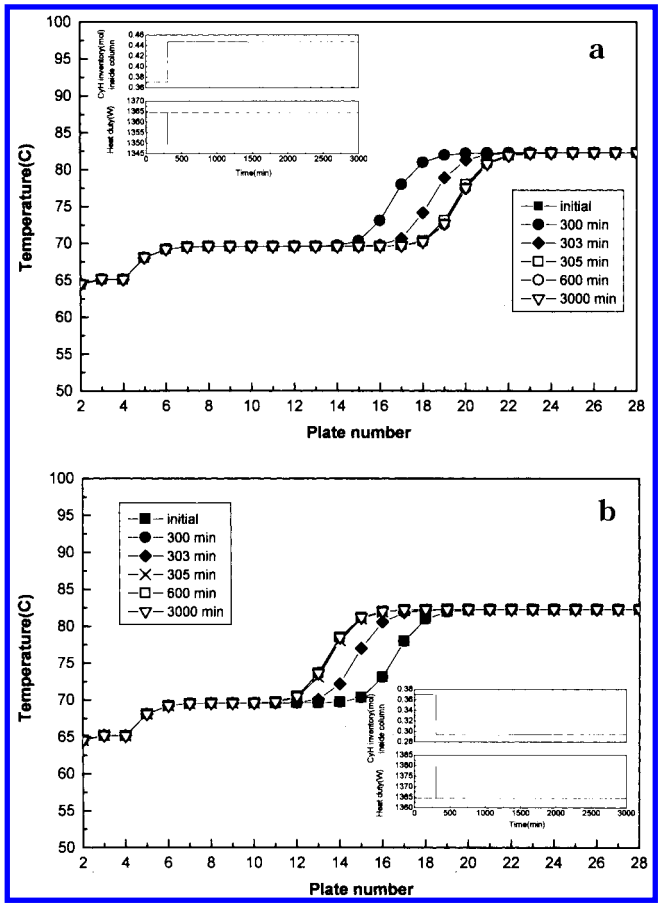

Figure 8. Shift of temperature front and entrainer inventory inside the column for a short pulse of (a) −15 W and (b) +15 W.

Obviously, steady states II and V are desired operations. The bottom IPA purity of both operations is quite high. However, the impurity in steady state II is mainly cyclohexane while that of steady state V is mainly water. Steady state II is easily identified by its temperature profile that has a plateau at 69.3 °C (the boiling point of the IPA + CyH azeotrope). Steady state V could be identified by the fact that a substantial section at the top of the column has two liquid phases. Both steady states exhibit parametric sensitivity with respect to reboiler duty.

It should be pointed out that the "hysteresis" phenomenon we reported between types I and II and types IV and V is different from the hysteresis between the upper high-purity stable branch and lower low-purity stable branch due to multiple steady states reported by Müller and Marquardt (1997). Rovaglio et al. (1993) found that it is important to control the amount of entrainer inside the column. Our operation strategy maintained a rough input−output balance of the entrainer, but there is no guarantee that the amount of entrainer inside the column is exactly constant. This explains the failure of the column to recover its original steady state after a series of step changes in reboiler duty. Using wave-propagation analysis, Kienle and Marquardt (1991) and Helfferich (1993) established that "creep" might occur for such systems. In Figure 8, short pulses of ±15 W and 5-min duration were given to the steady-state profile II at 1650 W at 300 min. Simulations were carried out to 3000 min. The temperature front was driven to different positions in the column. The entrainer inventory in the column holdup increased from 0.370 to 0.447 for a pulse of −15 W and decreased from 0.370 to 0.294 for a pulse of +15 W. No appreciable drift of the temperature front could be observed after a period of about 300 min. The entrainer inventory was stabilized to within 10^{-7}. The total residual of all 4 × 28 dynamic equations inside the column was found to be 10^{-6}. Our results seem to be consistent with the conclusion by Helfferich (1993) that, for a local equilibrium model, "... balance waves can stand at any positions making for infinite multiplicity".

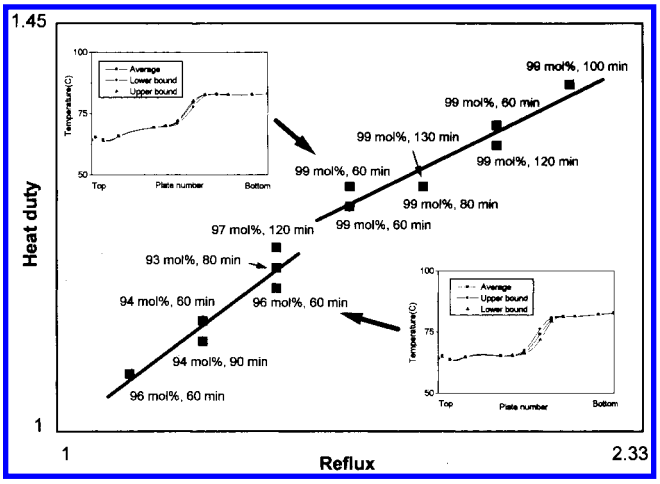

Figure 9. Experimental evidence for a critical reflux.

Experimental Confirmation of the Critical Reflux. An experiment was conducted in order to verify the existence of a critical reflux point. The feed was fixed at a constant rate and fed at the tenth plate from the top. Initially, a steady state with 69.3 °C plateau was started up at a high reflux and maintained for at least 60 min. Then the reflux was given a step decrease of 5 mL/min. The reboiler duty was then adjusted so that a temperature profile of desirable shape is sustained at least for 60 min. The bottom products at each steady state are sampled for GC analysis. The whole experiment together with initial startup and shutdown preparations usually took 6−8 h. In the next run, a steady state with the desired temperature profile was started up again at the reduced reflux of the previous run. The reboiler duty was then adjusted so that the same temperature profile was found and sustained for at least 60 min for reproducibility. The reflux was then given another step reduction of 5 mL/min, and the procedure was repeated. The results were presented in Figure 9. Type II and V profiles could only be found in a narrow region along the two straight lines shown. The intersection of the two lines is our critical reflux. A type II profile with 69.3 °C plateau will transform into a type V profile that does not have the plateau at 69.3 °C or vice versa when the system passes through this critical point. The plateau at 69.3 °C of the type II profile ensures that there is sufficient entrainer in the column for removing water. The trace impurity at the bottom contained a significant amount of cyclohexane. A type V profile is characterized by the observation that a lot of stages in the top section of the column become oily, an evidence of liquid−liquid separation. The trace impurity at the bottom contained mainly water but little cyclohexane. A substantial reduction in the mole fraction of IPA was observed.

Experimental Confirmation of Parametric Sensitivity and Hysteresis. Two experiments, one at a higher reflux and the other at a lower reflux, were carried out to investigate transient behavior for the two

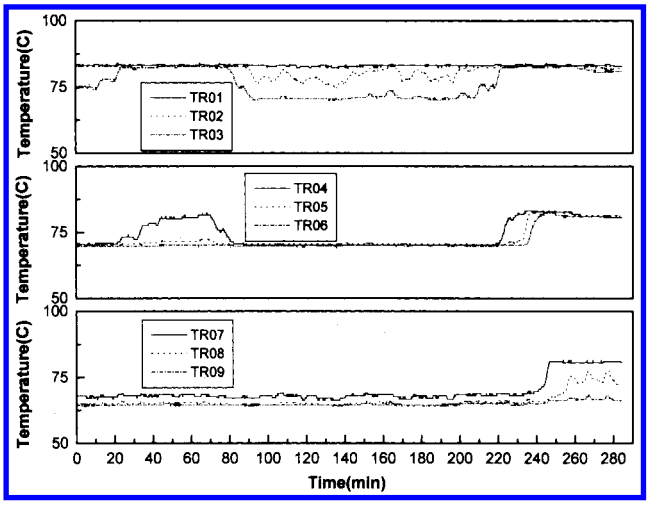

Figure 10. Experimental temperature responses at higher reflux.

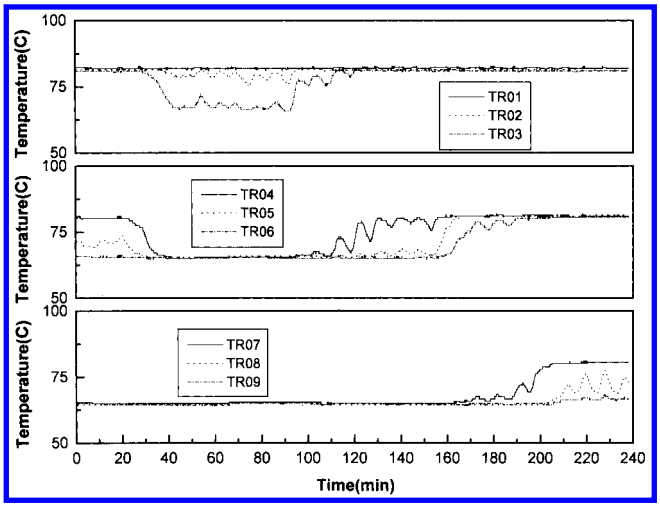

Figure 12. Experimental temperature responses at lower reflux.

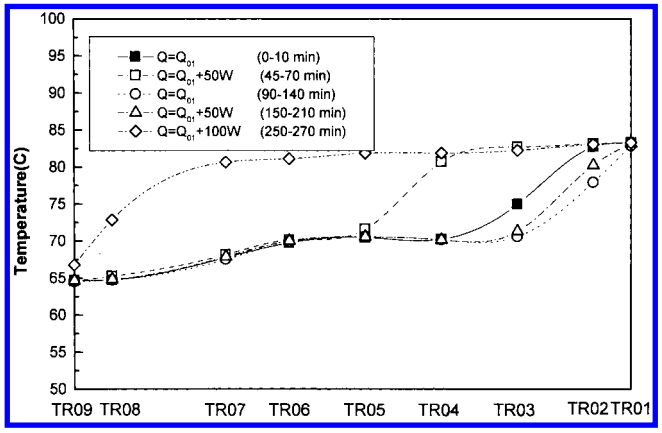

Figure 11. Experimental shifts in temperature profiles at higher reflux.

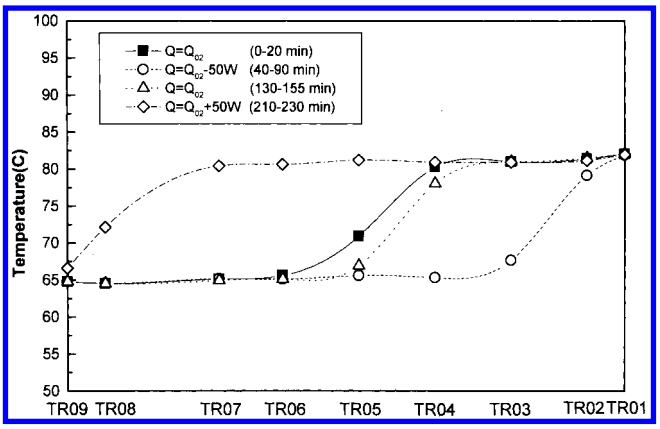

Figure 13. Experimental shifts in temperature profiles at lower reflux.

types of operation. Figure 10 is the temperature responses with respect to time for the case of the reflux rate corresponding value of 2.0 in Figure 9. After startup, an initial steady state is found at base value Q_{01}. TR04, TR05, and TR06 are at 69.3 °C. The temperature profile (Figure 11, 0−10 min) is of type II. At 10 min, we increase the reboiler duty by 50 W. The temperature front moved upward. The movement of the temperature front slowed around 45 min. This new profile consists of two plateaus, one at 83 °C at the bottom of the column and the other at 69.3 °C in the midsection. A type II was definitely obtained (Figure 11, 45−70 min). At 70 min, the reboiler duty is reduced by 50 W to the base value. The temperature front moved toward the bottom of the column. However, instead of settling into the original steady state, TR02 started to oscillate at 90 min. This oscillation was sustained for about 50 min. The average of the temperature profile during this period was shown in Figure 11 (90−140 min). It is a type I profile that is different from the initial profile obtained for the same duty. At 140 min, we increased the reboiler duty by 50 W. The temperature front moved slightly upward but remained oscillatory. We again let this oscillation be sustained for about 60 min. The average of the temperature profile during this period (Figure 11, 150−210 min) was found also to be a type I profile. At 210 min, we increase the reboiler duty again by 50 W. The temperature moved upward. After 40 min, the temperature front settled into a profile that is oscillating at TR07, TR08, and TR09. The average of this is similar to type III. The condition of the liquid at the top of the column was constantly monitored. Liquid-phase splitting can be found in the decanter only. The experimental results show that, at high reflux, a plateau at 69.3 °C can be established. The temperature front from 69.3 to 83 °C can be made to stand at various positions of the column within a 50-W increase in the reboiler duty. If the reboiler duty is increased by 100 W, the plateau at 69.3 °C disappears and the column will have a type III profile.

In the second experiment, the reflux was set at a lower value (corresponding to a value of 1.33 in Figure 9). The dynamic responses after the initial startup are shown in Figure 12. The reboiler duty was gradually increased to establish an initial steady state at base value Q_{02}. This steady state is similar to that of type V in our simulation (Figure 13, 0−20 min) with no plateau at 69.3 °C. Liquid-phase splitting can be found in the top plates down to TR08. At around 20 min, we reduced the reboiler duty by 50 W. The temperature front moved toward the bottom of the column and started to oscillate. This oscillating state was sustained for 50 min. The average temperature profile is similar to the one of type IV (Figure 13, 40−90 min). Then the reboiler duty is increased by 50 W back to original value. The temperature front oscillated but moved upward for 40 min. It remained oscillatory at TR04, TR05, and TR06 but maintained a relatively fixed average position for about 25 min. The average temperature has a type V profile (Figure 13, 130−155 min) but did not fully recover to the initial profile. A further increase of the

reboiler duty by 50 W led to an upward transient. The temperature front now oscillated at TR07, TR08, and TR09. The average profile is that of type III. During the last period when the system has been driven to a type III profile, liquid-phase splitting in the top section of the column disappears.

The failure of the system to recover to the original steady state was observed in dynamic simulation. It can be attributed to the fact that the amount of entrainer in the column changes. However, dynamic simulation did not produce the oscillatory response accompanying step changes in the reboiler duty. Rovaglio and Doherty (1990) found that small changes in pressure of the column might produce unexpected fluctuation in temperature and composition. However, the pressure drop of the column is monitored only manually and occasionally to prevent flooding. Without continuous pressure drop measurement, we cannot conveniently observe the changes in pressure nor the vapor load during the experimental runs. There are also variations in the feed flow rate and reflux flow. The main cause of oscillatory response remained unconfirmed.

It should be pointed out that we do not actually have direct experimental evidence of output steady-state multiplicity, although the experiment results were well supported by the bifurcation analysis. If we have reduced the heat duty after a type III profile was achieved, we could possibly have more direct experimental evidence of output steady-state multiplicity as demonstrated in dynamic simulation. Müller and Marquardt (1997) have furnished this kind of evidence for their system ethanol + cyclohexane + water.

Conclusion

In this work, the steady-state and dynamic behavior of a heterogeneous azeotropic IPA + CyH + H_2O column was investigated theoretically and experimentally. For a given reflux rate, two stable branches of steady-state solutions, one with high purity and the other with essentially no separation, were found at different reboiler duties. Therefore, for a given reflux there is a highest attainable purity corresponding to a given specific heat duty or vapor boilup rate. Heat duty increased beyond this point results in a catastrophic loss in IPA purity. At higher reflux, the temperature profile of the column with highest attainable purity passes around the IPA + CyH azeotrope characterized by a plateau at 69.3 °C. The bottom impurity is mainly cyclohexane. The purity does not change much as the reflux rate decreases until a critical reflux rate. Below this reflux, the temperature profile of the column at the end of the high-purity branch passes around the IPA + H_2O azeotrope. A lot of stages at the top have heterogeneous liquid splitting. The plateau at 69.3 °C disappears, and the bottom impurity is mainly water. Furthermore, the purity of IPA decreases substantially if the reflux rate is reduced. Both types of profiles demonstrate parametric sensitivity and multiple steady states. The critical reflux point represents an operating state that achieves high IPA purity with minimum energy consumption. In both high and low reflux regions, at given reflux and reboiler duty, the temperature profile that achieves a meaningful separation is not unique. The temperature front can be made to stand at different positions inside the column with a cyclic change in reboiler duty along the high-purity branch. This hysteresis phenomenon can be attributed to changes in the amount of entrainer in the column.

Acknowledgment

This work is partially supported by the National Science Council of the Republic of China under Grant NSC86-2214-E-182-005.

Nomenclature

Alphabets

a, b, c = coefficients for the Antoine equation
$h(H)$ = liquid (vapor) enthalpies, J/mol
K = equilibrium constant
L = liquid flow rate, mol/min
M = liquid holdup, mol
P^s = saturated vapor pressure, bar
T = temperature, K
x = liquid composition
y = vapor composition

Greek Symbols

β = phase fraction of organic phase
ξ = dimensionless time

Superscripts

$'$ = organic phase
$''$ = aqueous phase
$\bar{}$ = average properties of two coexisting liquid phases

Subscripts

i = species index
j = stage number

Literature Cited

Bekiaris, N.; Meski, G. A.; Radu, C. M.; Morari, M. Multiple Steady States in Homogeneous Azeotropic Distillation. *Ind. Eng. Chem. Res.* **1993**, *32*, 2023.

Bekiaris, N.; Meski, G. A.; Morari, M. Multiple Steady States in Heterogeneous Azeotropic Distillation. *Ind. Eng. Chem. Res.* **1996**, *35*, 207.

Bender, E.; Block, U. *Verfahrenstechnik* **1975**, *9*, 106.

Cairns, B. P.; Furzer, I. A. Multicomponent Three-Phase Azeotropic Distillation. 1. Extensive Experimental Data and Simulation Results. *Ind. Eng. Chem. Res.* **1990a**, *29*, 1349.

Cairns, B. P.; Furzer, I. A. Multicomponent Three-Phase Azeotropic Distillation. 2. Phase-Stability and Phase-Splitting Algorithms. *Ind. Eng. Chem. Res.* **1990b**, *29*, 1364.

Cairns, B. P.; Furzer, I. A. Multicomponent Three-Phase Azeotropic Distillation. 3. Modern Thermodynamic Models and Multiple Solutions. *Ind. Eng. Chem. Res.* **1990c**, *29*, 1383.

Doedel, E. J.; Wang, X. *AUTO94: Software for Continuation and Bifurcation Problems in Ordinary Differential Equations*; Computer Science Department of Concodia University: Montreal, Canada, 1994.

Gmehling, J.; Onken, U. *Vapor−Liquid Equilibrium Data Collection*; Chemistry Data Series; DECHEMA: Frankfurt, Germany, 1977.

Güttinger, T. E.; Dorn, C.; Morari, M. Experimental Study of Multiple Steady States in Homogeneous Azeotropic Distillation. *Ind. Eng. Chem. Res.* **1997**, *36*, 794.

Helfferich, F. G. Multiple Steady States in Multicomponent Countercurrent Mass-Transfer Processes. *Chem. Eng. Sci.* **1993**, *48*, 681.

Kienle, A.; Marquardt, W. Bifurcation Analysis of Multicomponent, Nonequilibrium Distillation Processes. *Chem. Eng. Sci.* **1991**, *46*, 1757.

Kovach, J. W., III; Seider, W. D. Heterogeneous Azeotropic Distillation: Experimental and Simulation Results. *AIChE J.* **1987a**, *33*, 1300.

Kovach, J. W., III; Seider, W. D. Heterogeneous Azeotropic Distillation: Homotopy-Continuation Methods. *Comput. Chem. Eng.* **1987b**, *11*, 593.

Magnussen, T.; Michelsen, M. L.; Fredenslund, A. Azeotropic Distillation Using UNIFAC. *Inst. Chem. Eng. Symp. Ser.* **1979**, *56*, 1.

Michelsen, M. L. The Isothermal Flash Problem, Part I: Stability. *Fluid Phase Equilib.* **1982**, *9*, 1.

Müller, D.; Marquardt, W. Experimental Verification of Multiple Steady States in Heterogeneous Azeotropic Distillation. *Ind. Eng. Chem. Res.* **1997**, *36*, 5410.

Müller, D.; Marquardt, W.; Hauschild, T.; Ronge, G.; Steude, H. Experimental Validation of an Equilibrium Stage Model for Three-Phase Distillation. *Inst. Chem. Eng. Symp. Ser.* **1997**, *142*, 149.

Pham, H. N.; Doherty, M. F. Design and Synthesis of Azeotropic Distillation: II. Residue Curve Maps. *Chem. Eng. Sci.* **1990**, *45*, 1837.

Pham, H. N.; Ryan, P. J.; Doherty, M. F. Design and Minimum Reflux for Heterogeneous Azeotropic Distillation Columns. *AIChE J.* **1989**, *35*, 1585.

Prokopakis, G. J.; Seider, W. D. Feasible Specifications in Azeotropic Distillation. *AIChE J.* **1983a**, *29*, 49.

Prokopakis, G. J.; Seider, W. D. Dynamic Simulation of Azeotropic Distillation Towers. *AIChE J.* **1983b**, *29*, 1017.

Prokopakis, G. J.; Ross, B. A.; Seider, W. D. Azeotropic Distillation Tower with Two Liquid Phases. In *Foundation of Computer-aided Chemical Process Design*; Mah, R. S. H., Seider, W. D., Eds.; AIChE: New York, 1981.

Reid, R. C.; Prausnitz, J. M.; Poling, B. E. *Properties of Gases and Liquids*, 4th ed.; McGraw-Hill: New York, 1988.

Rovaglio, M.; Doherty, M. F. Dynamics of Heterogeneous Distillation Columns. *AIChE J.* **1990**, *36*, 39.

Rovaglio, M.; Faravelli, T.; Biardi, G.; Gaffuri, P.; Soccol, S. The Key Role of Entrainer Inventory for Operation and Control of Heterogeneous Azeotropic Distillation Towers. *Comput. Chem. Eng.* **1993**, *17*, 535.

Schuil, J. A.; Bool, K. K. Three-phase Flash and Distillation. *Comput. Chem. Eng.* **1985**, *9*, 295.

Sørensen, J. M.; Arlt, W. *Liquid−Liquid Equilibrium Data Collection*; Chemistry Data Series; DECHEMA: Frankfurt, Germany, 1979.

Verhoeye, L. A. J. The System Cyclohexane−2-Propanol−Water. *J. Chem. Eng. Data* **1968**, *13*, 462.

Widagdo, S.; Seider, W. D. Azeotropic Distillation. *AIChE J.* **1996**, *42*, 96.

Widagdo, S.; Seider, W. D.; Sebastian, D. H. Bifurcation Analysis in Heterogeneous Azeotropic Distillation. *AIChE J.* **1989**, *35*, 1457.

Widagdo, S.; Seider, W. D.; Sebastian, D. H. Dynamic Analysis of Heterogeneous Azeotropic Distillation. *AIChE J.* **1992**, *38*, 1229.

Wong, D. S. H.; Jang, S. S.; Chang, C. F. Simulation of Dynamics and Phase Pattern Changes for an Azeotropic Distillation Column. *Comput. Chem. Eng.* **1991**, *15*, 325.

Received for review November 14, 1997
Revised manuscript received March 6, 1998
Accepted March 9, 1998

IE970855T